



HAL
open science

Gyrofluid modeling and phenomenology of low- β e Alfvén wave turbulence

T. Passot, P. Sulem, E. Tassi

► **To cite this version:**

T. Passot, P. Sulem, E. Tassi. Gyrofluid modeling and phenomenology of low- β e Alfvén wave turbulence. *Physics of Plasmas*, 2018, 25 (4), pp.042107. 10.1063/1.5022528 . hal-02072460

HAL Id: hal-02072460

<https://hal.science/hal-02072460>

Submitted on 1 Feb 2022

HAL is a multi-disciplinary open access archive for the deposit and dissemination of scientific research documents, whether they are published or not. The documents may come from teaching and research institutions in France or abroad, or from public or private research centers.

L'archive ouverte pluridisciplinaire **HAL**, est destinée au dépôt et à la diffusion de documents scientifiques de niveau recherche, publiés ou non, émanant des établissements d'enseignement et de recherche français ou étrangers, des laboratoires publics ou privés.

Gyrofluid modeling and phenomenology of low- β_e Alfvén wave turbulence

T. Passot¹, P.L. Sulem¹ and E. Tassi^{1,2}

¹ *Université Côte d'Azur, CNRS, Observatoire de la Côte d'Azur, Laboratoire J.L. Lagrange, Boulevard de l'Observatoire, CS 34229, 06304 Nice Cedex 4, France*

² *Aix Marseille Univ, Univ Toulon, CNRS, CPT, 13288 Marseille, France*

A two-field reduced gyrofluid model including electron inertia, ion finite Larmor radius corrections and parallel magnetic field fluctuations is derived from the model of Brizard (Phys. Fluids B **4**, 1213 (1992)). It assumes low β_e , where β_e indicates the ratio between the equilibrium electron pressure and the magnetic pressure exerted by a strong uniform magnetic guide field, but permits an arbitrary ion-to-electron equilibrium temperature ratio. It is shown to have a noncanonical Hamiltonian structure and provides a convenient framework for studying kinetic Alfvén wave turbulence, from magnetohydrodynamics (MHD) to sub- d_e scales (where d_e holds for the electron skin depth). Magnetic energy spectra are phenomenologically determined within energy and generalized cross-helicity cascades in the perpendicular spectral plane. Arguments based on absolute statistical equilibria are used to predict the direction of the transfers, pointing out that, within the sub-ion range, the generalized cross-helicity could display an inverse cascade if injected at small scales, for example by reconnection processes.

PACS numbers: 94.05.-a, 52.30-q, 52.30.Ex, 52.65.Kj, 52.35.Bj, 47.10.Df 52.35.Ra, 52.35.Vd

I. INTRODUCTION

The turbulent dynamics of collisionless magnetized plasmas involves a large range of spatial and temporal scales, which interact with each other, even when widely separated. As an example, the global evolution of a shear flow (e.g. in the context of the solar wind-magnetosphere interaction) depends on the local reconnection events whose speed has been shown to play a major role [1]. This multi-scale character can become a real obstacle in three-dimensional numerical simulations, thus motivating the search for simple fluid or gyrofluid models containing the necessary physical ingredients but focusing on some specific aspects. In this paper, we are concerned with Alfvénic turbulence which is a main element of the dynamics of the solar wind, a medium often viewed as a natural laboratory for collisionless plasma turbulence, thanks to the high-quality of in situ data obtained by Earth orbiting spacecrafts. Special attention will be paid to the turbulence properties in the sub-ion range, a topic which is still actively debated [2–8]. A study of this regime needs a model capable of describing a wide domain of scales, from those associated with the classical MHD Alfvén wave cascade (thus larger than the ion inertial length d_i) to those at which collisionless magnetic reconnection typically takes place, i.e. a fraction of the electron inertial length d_e . The model should be able to properly reproduce the linear properties of kinetic Alfvén waves (KAWs), and should thus retain the parallel magnetic field fluctuation B_z . It should furthermore be valid for a large range of values of the ion to electron equilibrium temperature ratio $\tau = T_{0i}/T_{0e}$, and thus include a description of ion finite Larmor radius (FLR) corrections. To keep the model simple enough, electron FLR corrections should be excluded, thus limiting the considered scales to those larger than the electron

Larmor radius ρ_e . Retaining scales of order d_e , while excluding those approaching ρ_e , thus limits the model to small enough values of the electron beta parameter β_e . As we shall see, β_e will typically be assumed of the order of $\delta = (m_e/m_i)^{1/2}$ where m_e and m_i stand for the mass of the electrons and the ions (here taken to be protons), respectively. A small β_e regime, although observed in the solar wind near the Earth [9], is more often encountered closer to the Sun or in the solar corona. Nevertheless, studying the nonlinear phenomena predicted by this model should shed light on the dynamics in more general situations. It should also be desirable to focus the description on the minimum number of fields necessary to describe KAWs, thus excluding the coupling to other waves (such as fast and slow magnetosonic ones), as long as the latter are not driven by the KAW dynamics. Finally, it is important to require that the resulting model could be cast in Hamiltonian form so that, in the absence of explicit energy sinks, necessary in a turbulent framework, no unphysical dissipation takes place, that could otherwise, for instance, alter the triggering of magnetic reconnection.

Many reduced fluid and/or gyrofluid models already exist to describe magnetic reconnection and/or Alfvénic turbulence. The simplest fluid model to describe KAWs, which is limited to sub-ion scales and discards electron inertia, is a two-field system derived in Ref. [10] and studied in Ref. [11]. Fluid models including B_z and electron inertia have also been derived, but are limited to specific ranges of τ . Indeed, a fluid computation of ion FLR corrections restricts the considered scales to be either much larger than the ion Larmor radius ρ_i (for which a perturbative approach is possible) or much smaller than ρ_i , a case where the ion velocity is negligible. When concentrating on scales of the order of the sonic Larmor radius ρ_s , defined as $\rho_s = \rho_i/\sqrt{2\tau}$, these regimes correspond to a value of τ either much smaller or much larger than unity,

respectively. The case of negligible τ was addressed in two dimensions in Refs. [12, 13] and extended to three dimensions in Ref. [14]. The case where τ is small but not totally negligible (or finite, provided the considered scales are assumed larger than ρ_i) was addressed in Ref. [15], but in this case electron inertia was neglected. The cases $\tau \gtrsim 1$ or $\tau \gg 1$ were studied in Ref. [16], in a situation where electron inertia and FLRs were retained. The latter case $\tau \gg 1$ was also addressed in Ref. [17] (note that electron FLRs are neglected in this reference). A review of reduced fluid models that can be derived from a gyrokinetic approach can be found in Ref. [10].

The more general case of finite τ can only be addressed using a gyrofluid approach. In this framework, a simple model for Alfvénic turbulence was obtained in Ref. [18], neglecting electron inertia and parallel magnetic fluctuations. Many gyrofluid models with electron inertia have been derived and studied in the context of collisionless reconnection, after the pioneering work of Ref. [19]. Nevertheless, almost none of them includes the parallel magnetic fluctuations B_z .

The first aim of this paper is to apply an asymptotic ordering, starting from the general model (hereafter referred to as parent model) given in Ref. [20], in order to derive a reduced gyrofluid model satisfying the requirements mentioned above. The adopted asymptotic ordering leads to neglecting the coupling to the parallel ion velocity u_i , and thus to the slow magnetosonic modes (actually damped by Landau resonance). The final model is a two-field model and possesses a noncanonical Hamiltonian structure.

Another aim of this paper is to use this two-field gyrofluid model to study phenomenologically critically-balanced KAW turbulence at scales ranging from MHD to sub- d_e scales, paying a special attention to the transverse magnetic energy spectra in the energy or the generalized cross-helicity cascade, and to the direct or inverse character of these cascades. Such Kolmogorov-like phenomenology dismisses the possible effect of coherent structures such as current sheets which form as the result of the turbulent MHD cascade and which, in some instances, can be destabilized by magnetic reconnection. Recent two-dimensional hybrid-kinetic simulations [21] suggest that, in the non-collisional regime, this process is fast enough to compete with the wave mode interactions, in a way that could affect the cascade at scales comparable to the ion inertial length d_i , typical of the current sheet width. In a small β_i plasma, where $\beta_i = \tau\beta_e$, this scale is significantly larger than ρ_s , and the spectral break can indeed take place at d_i , as suggested by other recent two-dimensional hybrid simulations [22]. The above gyrofluid model can provide an efficient tool to address this issue.

The paper is organized as follows. The derivation of the reduced gyrofluid model is presented in Section II. Its application to a phenomenological study of critically-balanced KAW turbulence is performed in Sect. III. Section IV presents a short summary together with a few

comments. In Appendix A, the parent gyrofluid model is presented. In Appendix B, an alternative derivation of the electron equations which a priori ensures the Hamiltonian structure of the model is presented.

II. A GYROFLUID MODEL FOR ALFVÉN WAVES

A. The characteristic scales

Before presenting the derivation of the model, it is useful to order the various relevant scales estimated in a homogeneous equilibrium state characterized by a density n_0 , isotropic ion and electron temperatures T_{0i} and T_{0e} , and subject to a strong ambient magnetic field of amplitude B_0 along the z -direction. In terms of the sonic Larmor radius $\rho_s = c_s/\Omega_i$, where $c_s = \sqrt{T_{0e}/m_i}$ is the sound speed and $\Omega_i = eB_0/(m_i c)$ the ion gyrofrequency, one has

$$\begin{aligned} d_i &= \sqrt{\frac{2}{\beta_e}} \rho_s, & d_e &= \sqrt{\frac{2}{\beta_e}} \delta \rho_s, \\ \rho_i &= \sqrt{2\tau} \rho_s, & \rho_e &= \sqrt{2} \delta \rho_s, \end{aligned} \quad (1)$$

where $\beta_e = 8\pi n_0 T_{0e}/B_0^2$, $\delta^2 = m_e/m_i$ and $\tau = T_{0i}/T_{0e}$. We have here defined the particle Larmor radii ($r = i$ for the ions, $r = e$ for the electrons) by $\rho_r = v_{thr}/\Omega_r$, where the particle thermal velocities are given by $v_{thr} = (2T_r/m_r)^{1/2}$, the cyclotron frequencies by $\Omega_r = eB_0/(m_r c)$ and the inertial lengths by $d_r = v_A/\Omega_r$ where $v_A = B_0/(4\pi n_0 m_i)^{1/2} = c_s \sqrt{2/\beta_e}$ is the Alfvén velocity. The relative magnitude of the characteristic scales is also exemplified for various values of β_e and τ in the top label of Figs. 2 to 4.

The model to be derived should cover a spectral range which includes both scales large compared to d_i (typical of the width of the generated current sheets) and scales comparable to d_e (typical of collisionless reconnection processes). The considered scales will also be assumed to remain large compared to ρ_e . This in particular implies the condition that $\rho_e/d_e = \beta_e^{1/2}$ be small enough.

It is convenient to take the sonic Larmor radius ρ_s , the sound speed c_s and the inverse ion gyrofrequency Ω_i^{-1} as length, velocity and time units, and to use nondimensional variables, as defined in Appendix A. The magnitude of the electric potential φ is controlled by the parameter $\varepsilon \ll 1$, as $\varphi = O(\varepsilon)$. We assume that at scale ρ_s , $\partial_t = O(\varepsilon)$ and $\nabla_\perp \sim O(1)$. We denote by A_\parallel the parallel component of the magnetic potential, by N_e and U_e the gyrocenter electron and parallel velocity respectively, and by B_z the longitudinal magnetic field fluctuations. The magnetic field thus reads to leading order $\mathbf{B} = \nabla A_\parallel \times \hat{z} + B_z \hat{z}$.

B. Derivation of the model

We consider as starting point the gyrofluid system (A3)-(A14) originating from Ref. [20], which allows considering all the values of the ion-to-electron temperature ratio. It is one of the rare gyrofluid models that accounts for parallel magnetic perturbations (a crucial ingredient to describe KAWs) and permits considering a higher β_e regime. Other low- β_e gyrofluid models, such as those of Refs. [23, 24], adopt different closures for the gyroaveraging operators, compared to Ref. [20], which are more precise at scales close to the ion gyroradius. It however turns out that these gyroaveraging operators only affect the evolution of ion quantities (gyrocenter density, parallel velocity and temperatures) which do not enter the final two-field model derived in the present paper. The ion FLR corrections present in the gyrokinetic Poisson equation and in Ampere's law, on the other hand, take the same form in all these models.

The two-field model we derive here allows one to focus on Alfvén wave dynamics, neglecting the coupling with slow magnetosonic waves. It retains corrections associated with electron inertia as well as an electron FLR contribution which becomes relevant when the temperature ratio τ is larger than $1/\beta_e$. As shown below, the large τ case is obtained by choosing a scaling where $\tau \sim 1/\delta$, but the resulting equations remain valid for even larger values of τ .

Considering the KAW dynamics for the assumed values of β_e , Landau damping is efficient enough to homogenize electron temperatures along the magnetic field lines. When neglecting dissipation phenomena, assuming fully isothermal electrons is in fact a good approximation (see also Ref. [25] and the simulations of Ref. [26]). The first step in the derivation of the two-field model from the parent model (A3)-(A14) thus consists in assuming an isothermal closure for the electron fluid. We denote with $T_{\parallel r} = P_{\parallel r} - N_r$ and $T_{\perp r} = P_{\perp r} - N_r$ the parallel and perpendicular gyrocenter temperatures of the species r . In terms of gyrocenter moments, the electron isothermal assumption, as deduced from Eqs. (3.68a)-(3.69b) of Ref. [25], corresponds to imposing $T_{\parallel e} = 0$ and $T_{\perp e} = -B_z$. These two relations will then replace the evolution equations (A6) and (A7) of the parent model. A further assumption is that of a non-relativistic Alfvén speed (i.e. $v_A \ll c$), which allows us to neglect the first term on the left-hand side of Eq. (A12), thus turning Poisson's equation into a quasi-neutrality relation.

The derivation then proceeds by considering two expansion parameters

$$\delta \ll 1, \quad \varepsilon \ll 1, \quad (2)$$

and introducing two scalings, denoted as scaling I and scaling II. Asymptotic reductions of the parent model according to the two scalings is carried out in the following way. We first consider scaling I, which is given by

$$\beta_e = O(\delta), \quad \tau \sim \nabla_{\perp} = O(1), \quad (3)$$

$$U_e \sim Q_{\perp e} = O\left(\frac{\varepsilon}{\delta^{1/2}}\right), \quad A_{\parallel} \sim \partial_z = O(\delta^{1/2}\varepsilon), \quad (4)$$

$$\partial_t \sim N_e \sim \varphi \sim N_i \sim T_{\perp i} \sim T_{\parallel i} = O(\varepsilon), \quad (5)$$

$$B_z \sim U_i \sim Q_{\perp i} \sim Q_{\parallel i} \sim R_{\parallel i} \sim R_{\perp i} = O(\delta\varepsilon). \quad (6)$$

We impose such scaling to the parent equations (A3), (A5), (A8)-(A14) and retain leading order terms in ε and δ , as well as first-order corrections in δ , in each equation. The resulting system reads

$$\frac{\partial N_e}{\partial t} + [\varphi, N_e] - [B_z, N_e] + \nabla_{\parallel} U_e = 0, \quad (7)$$

$$\frac{\partial}{\partial t}(\delta^2 U_e - A_{\parallel}) + [\varphi, \delta^2 U_e - A_{\parallel}] + \nabla_{\parallel}(N_e + B_z) - \frac{\partial \varphi}{\partial z} = 0, \quad (8)$$

$$\begin{aligned} \frac{\partial N_i}{\partial t} + [e^{\tau \Delta_s} \varphi, N_i] + \tau[\Delta_s e^{\tau \Delta_s} \varphi, T_{\perp i}] \\ + \tau[e^{\tau \Delta_s} B_z, P_{\perp i}] + \tau^2[\Delta_s e^{\tau \Delta_s} B_z, T_{\perp i}] = 0, \end{aligned} \quad (9)$$

$$\begin{aligned} \frac{\partial P_{\parallel i}}{\partial t} + [e^{\tau \Delta_s} \varphi, P_{\parallel i}] + \tau[\Delta_s e^{\tau \Delta_s} \varphi, T_{\perp i}] \\ + \tau[e^{\tau \Delta_s} B_z, P_{\parallel i} + T_{\perp i}] \\ + \tau^2[\Delta_s e^{\tau \Delta_s} B_z, T_{\perp i}] = 0, \end{aligned} \quad (10)$$

$$\begin{aligned} \frac{\partial P_{\perp i}}{\partial t} + [(1 + \tau \Delta_s) e^{\tau \Delta_s} \varphi, P_{\perp i}] \\ + \tau[\Delta_s(2 + \tau \Delta_s) e^{\tau \Delta_s} \varphi, T_{\perp i}] \\ + \tau[(2 + \tau \Delta_s) e^{\tau \Delta_s} B_z, 2P_{\perp i} - N_i] \\ + \tau^2[\Delta_s(3 + \tau \Delta_s) e^{\tau \Delta_s} B_z, T_{\perp i}] = 0, \end{aligned} \quad (11)$$

$$\begin{aligned} 0 = N_e + (1 - \tilde{\Gamma}_0 + \tilde{\Gamma}_1) B_z - e^{\tau \Delta_s} N_i \\ - \tau \Delta_s e^{\tau \Delta_s} T_{\perp i} - \frac{(\tilde{\Gamma}_0 - 1)}{\tau} \varphi, \end{aligned} \quad (12)$$

$$\Delta_{\perp} A_{\parallel} = \frac{\beta_e}{2} U_e, \quad (13)$$

$$\begin{aligned} B_z = -\frac{\beta_e}{2}(P_{\perp e} - \varphi + 2B_z + \tau e^{\tau \Delta_s} P_{\perp i} + \tau^2 \Delta_s e^{\tau \Delta_s} T_{\perp i} \\ + (\tilde{\Gamma}_0 - \tilde{\Gamma}_1) \varphi + 2\tau(\tilde{\Gamma}_0 - \tilde{\Gamma}_1) B_z). \end{aligned} \quad (14)$$

Here, $[f, g] = (\partial_x f \partial_y g - \partial_y f \partial_x g)$ denotes the canonical bracket of two scalar functions f and g . Furthermore, $\tilde{\Gamma}_n$ denotes the (non-local) operator $\Gamma_n(-\tau \Delta_{\perp})$ associated with the Fourier multiplier $\Gamma_n(\tau k_{\perp}^2)$, defined by $\Gamma_n(x) = I_n(x) e^{-x}$ where I_n is the modified Bessel function of first type of order n . The parallel gradient operator ∇_{\parallel} , on the other hand, is defined by

$$\nabla_{\parallel} f = -[A_{\parallel}, f] + \frac{\partial f}{\partial z}, \quad (15)$$

for a function f . We remark that, as a consequence of the scaling, U_i gets decoupled from the system. Consequently, we do not include its evolution equation in the system. On the other hand, we observe that we can take $N_i = T_{\parallel i} = T_{\perp i} = 0$ as solutions for Eqs. (9), (10) and (11), and replace such solutions in the remaining equations.

An analogous asymptotic reduction is then carried out based on scaling II, which reads

$$\beta_e = O(\delta), \quad \tau = O(1/\delta), \quad \nabla_{\perp} = O(1), \quad (16)$$

$$U_e \sim Q_{\perp e} = O\left(\frac{\varepsilon}{\delta^{1/2}}\right), \quad \partial_t \sim \varphi = O(\varepsilon), \quad (17)$$

$$A_{\parallel} \sim \partial_z = O(\delta^{1/2}\varepsilon), \quad (18)$$

$$N_e \sim B_z \sim N_i \sim T_{\perp i} \sim T_{\parallel i} \sim U_i \sim Q_{\perp i} \sim Q_{\parallel i} \quad (19)$$

$$\sim R_{\parallel \perp i} \sim R_{\perp \perp i} = O(\delta\varepsilon). \quad (20)$$

Scaling II accounts for corrections relevant for large τ but requires smaller electron gyrocenter density fluctuations.

The asymptotically reduced system based on scaling II reads

$$\frac{\partial N_e}{\partial t} + [\varphi, N_e] + \nabla_{\parallel} U_e = 0, \quad (21)$$

$$\begin{aligned} \frac{\partial}{\partial t}(\delta^2 U_e - A_{\parallel}) + [\varphi, \delta^2 U_e - A_{\parallel}] + \nabla_{\parallel}(N_e + B_z) \\ - \frac{\partial \varphi}{\partial z} = 0, \end{aligned} \quad (22)$$

$$\frac{\partial N_i}{\partial t} + \frac{\partial U_i}{\partial z} = 0, \quad (23)$$

$$\frac{\partial U_i}{\partial t} + \tau[B_z, Q_{\perp i}] + \tau \frac{\partial P_{\parallel i}}{\partial z} = 0, \quad (24)$$

$$\frac{\partial P_{\parallel i}}{\partial t} + \tau[B_z, R_{\parallel \perp i}] + \nabla_{\parallel} Q_{\parallel i} + 3 \frac{\partial U_i}{\partial z} = 0, \quad (25)$$

$$\frac{\partial P_{\perp i}}{\partial t} + 2\tau[B_z, R_{\perp \perp i}] + \nabla_{\parallel} Q_{\perp i} + \frac{\partial U_i}{\partial z} = 0, \quad (26)$$

$$0 = N_e - 2\delta^2 \Delta_s \varphi + B_z + \frac{\varphi}{\tau}, \quad (27)$$

$$\Delta_{\perp} A_{\parallel} = \frac{\beta_e}{2} U_e, \quad (28)$$

$$B_z = -\frac{\beta_e}{2}(P_{\perp e} - \varphi + 2B_z). \quad (29)$$

Note that, due to the large τ assumption, the ion gyroaveraged terms are subdominant in this scaling (we remark that, in the parent model, gyroaverage operators acting on the heat fluxes and energy-weighted pressure tensors are not taken into account). We can then take $N_i = U_i = T_{\parallel i} = T_{\perp i} = Q_{\parallel i} = Q_{\perp i} = R_{\parallel \perp i} = R_{\perp \perp i} = 0$ as solutions for Eqs. (23), (24), (25) and (26).

The final gyrofluid model is obtained by retaining all the terms in the reduced models resulting from the two scalings, as well as one correction of order δ^2 corresponding to the term $-\delta^2[B_z, U_e]$ which originates from Eq. (A5). This term, as will be seen a posteriori, allows the final system to be cast in Hamiltonian form. By means of this procedure, one is finally led to the following two-field model in the form of a continuity equation for the electron gyrocenter density, coupled to Ohm's law

$$\partial_t N_e + [\varphi, N_e] - [B_z, N_e] + \frac{2}{\beta_e} \nabla_{\parallel} \Delta_{\perp} A_{\parallel} = 0 \quad (30)$$

$$\partial_t \left(1 - \frac{2\delta^2}{\beta_e} \Delta_{\perp}\right) A_{\parallel} - [\varphi, \frac{2\delta^2}{\beta_e} \Delta_{\perp} A_{\parallel}] + [B_z, \frac{2\delta^2}{\beta_e} \Delta_{\perp} A_{\parallel}]$$

$$+ \nabla_{\parallel}(\varphi - N_e - B_z) = 0 \quad (31)$$

with

$$\begin{aligned} \left(\frac{2}{\beta_e} + (1 + 2\tau)(\tilde{\Gamma}_0 - \tilde{\Gamma}_1)\right) B_z = \\ \left(1 - \left(\frac{\tilde{\Gamma}_0 - 1}{\tau}\right) - \tilde{\Gamma}_0 + \tilde{\Gamma}_1\right) \varphi \end{aligned} \quad (32)$$

$$\begin{aligned} N_e = \left(\frac{\tilde{\Gamma}_0 - 1}{\tau} + \delta^2 \Delta_{\perp}\right) \varphi \\ - (1 - \tilde{\Gamma}_0 + \tilde{\Gamma}_1) B_z, \end{aligned} \quad (33)$$

deriving from Ampère's law and quasi-neutrality, respectively.

In Eq. (31), the term $[B_z, \frac{2\delta^2}{\beta_e} \Delta_{\perp} A_{\parallel}]$ is sub-dominant in both scalings I and II but, as mentioned above, it has been retained for it allows for a Hamiltonian formulation of the model in terms of a Lie-Poisson structure for the 2D limit, extended to 3D according to the procedure discussed in Ref. [14]. Interestingly the system conserves the energy, shown below to be given by Eq. (44), even in the absence of this term. We remark that, as shown in Appendix B, the model and its Hamiltonian structure can also be derived from a drift-kinetic equation, by prescribing the relations (32)-(33) and applying the procedure described in Ref. [27].

We also note that the second term on the right-hand side of the relation (33), which is proportional to δ^2 , corresponds to the above mentioned electron FLR correction, which is relevant when $\beta_i \sim 1$.

We note that when neglecting electron inertia, i.e. the δ^2 contributions, and introducing the ion and electron particle number densities n_i and n_e , expression (33) for N_e gives

$$n_i = n_e = N_e + B_z = \frac{\tilde{\Gamma}_0 - 1}{\tau} \varphi + (\tilde{\Gamma}_0 - \tilde{\Gamma}_1) B_z, \quad (34)$$

consistent with Eq. (B1) of Ref. [28], originating from the low-frequency linear kinetic theory taken in the regime of adiabatic ions (with the present scalings, $\zeta_i = \omega/(k_z v_{thi}) \gg 1$ and thus $R(\zeta_i) \ll 1$, where R is the plasma response function).

Substituting the expressions for N_e and B_z given by Eqs. (32) and (33) into Eqs. (30)-(31), the resulting model only involves the electric and magnetic potentials φ and A_{\parallel} .

C. Fluid limiting regimes

In the limit $\tau \ll 1$, where $N_e = \Delta_{\perp} \varphi$ and $B_z = -\frac{\beta_e/2}{1+\beta_e/2} \Delta_{\perp} \varphi$, and at large scales where electron inertia can be neglected, one recovers Eqs. (3.2)-(3.3) and (3.10)-(3.12) of Ref. [25] (under the same assumptions mentioned at the beginning of the present Section). In this limit, it is possible to consider a finite value of β_e .

If, on the other hand, electron inertia is kept into account, and β_e is taken small enough so as to neglect B_z contributions, Eqs. (30)-(31) lead to the two-field model of Refs. [19, 29] consisting of the following ion vorticity equation and Ohm's law:

$$\partial_t \Delta_{\perp} \varphi + [\varphi, \Delta_{\perp} \varphi] + \frac{2}{\beta_e} \nabla_{\parallel} \Delta_{\perp} A_{\parallel} = 0 \quad (35)$$

$$\begin{aligned} \partial_t \left(1 - \frac{2\delta^2}{\beta_e} \Delta_{\perp}\right) A_{\parallel} - [\varphi, \frac{2\delta^2}{\beta_e} \Delta_{\perp} A_{\parallel}] \\ + \nabla_{\parallel} (\varphi - \Delta_{\perp} \varphi) = 0. \end{aligned} \quad (36)$$

It also corresponds to the "low- β case" of the two-fluid model of Ref. [30], when restricted to 2D and when the electron pressure gradient in Ohm's law, usually referred to as parallel electron compressibility (term $\nabla_{\parallel} \Delta \varphi$ in Eq. (36)), is not retained.

When $\beta_i \sim 1$, one has (taking the limit $\tau \gg 1$) $B_z = \frac{\beta_e}{2} \varphi$ and $N_e = -\frac{\beta_e}{2} (1 + \frac{2}{\beta_i} - \frac{2\delta^2}{\beta_e} \Delta_{\perp}) \varphi$. After neglecting subdominant corrections proportional to β_e , the system reduces to

$$\begin{aligned} \partial_t \left(1 + \frac{2}{\beta_i} - \frac{2\delta^2}{\beta_e} \Delta_{\perp}\right) \varphi - [\varphi, \frac{2\delta^2}{\beta_e} \Delta_{\perp} \varphi] \\ - \frac{4}{\beta_e^2} \nabla_{\parallel} \Delta_{\perp} A_{\parallel} = 0 \end{aligned} \quad (37)$$

$$\begin{aligned} \partial_t \left(1 - \frac{2\delta^2}{\beta_e} \Delta_{\perp}\right) A_{\parallel} - [\varphi, \frac{2\delta^2}{\beta_e} \Delta_{\perp} A_{\parallel}] \\ + \nabla_{\parallel} \varphi = 0, \end{aligned} \quad (38)$$

which identifies with the isothermal system (5.9)-(5.10) of Ref. [16] taken for large values of τ when electron FLR corrections are neglected (see also Ref. [17]). This system, when restricted to 2D, in fact corresponds to the 2D electron MHD (EMHD) equations.

D. Hamiltonian structure

Similarly to many other reduced fluid and gyrofluid models (see Ref. [31] for a recent review), the system (30)-(31), as above mentioned, possesses a noncanonical Hamiltonian structure. In order to show this point, we first observe that the system (30)-(31) can be formulated as an infinite-dimensional dynamical system with the fields N_e and $A_e \equiv (1 - 2\delta^2 \Delta_{\perp} / \beta_e) A_{\parallel}$ as dynamical variables. Indeed, upon introducing the following positive definite operators

$$L_1 = \frac{2}{\beta_e} + (1 + 2\tau)(\tilde{\Gamma}_0 - \tilde{\Gamma}_1) \quad (39)$$

$$L_2 = 1 + \frac{1 - \tilde{\Gamma}_0}{\tau} - \tilde{\Gamma}_0 + \tilde{\Gamma}_1 \quad (40)$$

$$L_3 = \frac{1 - \tilde{\Gamma}_0}{\tau} - \delta^2 \Delta_{\perp} \quad (41)$$

$$L_4 = 1 - \tilde{\Gamma}_0 + \tilde{\Gamma}_1, \quad (42)$$

one can write $B_z = M_1 \varphi$, with $M_1 = L_1^{-1} L_2$, and $\varphi = -M_2^{-1} N_e$, where $M_2 = (L_3 + L_4 L_1^{-1} L_2)$ is positive definite, as numerically seen on its Fourier transform. Also, $A_{\parallel} = (1 - 2\delta^2 \Delta_{\perp} / \beta_e)^{-1} A_e$. Thus, B_z , φ and A_{\parallel} can be expressed in terms of the dynamical variables N_e and A_e .

Proving that the system possesses a Hamiltonian structure amounts to show that, given any observable F of the system, i.e. a functional of N_e and A_e , its evolution can be cast in the form [32]

$$\frac{\partial F}{\partial t} = \{F, \mathcal{H}\}, \quad (43)$$

where \mathcal{H} is an observable corresponding to the Hamiltonian functional and $\{, \}$ is a Poisson bracket.

For the system (30)-(31), the Hamiltonian is given by the conserved functional

$$\begin{aligned} \mathcal{H} = \frac{1}{2} \int \left(\frac{2}{\beta_e} |\nabla_{\perp} A_{\parallel}|^2 + \frac{4\delta^2}{\beta_e^2} |\Delta_{\perp} A_{\parallel}|^2 \right. \\ \left. - N_e (\varphi - N_e - B_z) \right) d^3 x, \end{aligned} \quad (44)$$

whereas the Poisson bracket reads

$$\begin{aligned} \{F, G\} = \int \left((N_e ([F_{N_e}, G_{N_e}] + \delta^2 [F_{A_e}, G_{A_e}]) \right. \\ \left. + A_e ([F_{N_e}, G_{A_e}] + [F_{A_e}, G_{N_e}]) \right. \\ \left. + F_{N_e} \partial_z G_{A_e} + F_{A_e} \partial_z G_{N_e} \right) d^3 x, \end{aligned} \quad (45)$$

for two observables F and G , subscripts on functionals denoting functional derivatives.

The Poisson bracket (45) corresponds, up to the normalization, to the Poisson bracket for the model of Ref. [19], when the latter is reduced to a two-field model by setting the ion density fluctuations proportional to vorticity.

E. Invariants

As is common with noncanonical Hamiltonian systems [32], the Poisson bracket (45) possesses Casimir invariants, corresponding to

$$C_{\pm} = \int G_{\pm} d^3 x, \quad (46)$$

where $G_{\pm} = A_e \pm \delta N_e$ are referred to as normal fields [33]. In terms of these fields, the system (30)-(31) rewrites in the form

$$\partial_t G_{\pm} + [\varphi_{\pm}, G_{\pm}] + \partial_z \left(\varphi_{\pm} \mp \frac{1}{\delta} G_{\pm} \right) = 0, \quad (47)$$

where $\varphi_{\pm} = \varphi - B_z \pm \frac{1}{\delta} A_{\parallel}$.

In the 2D limit with translational symmetry along z , the Poisson bracket, in terms of the variables G_{\pm} , takes

the form of a direct product and the system possesses two infinite families of Casimir invariants given by

$$C_{\pm} = \int \mathcal{C}_{\pm}(G_{\pm}) d^2x, \quad (48)$$

with \mathcal{C}_{\pm} arbitrary functions. In particular, one has the quadratic invariants $\int d^2x G_{\pm}^2$ which, in the limit of negligible electron inertia, lead to the classical conservation of the variance of the magnetic potential $\int d^2x A_{\parallel}^2$ of 2D MHD. In 2D, Eqs. (47) take the form of advection equations for the Lagrangian invariants G_{\pm} transported by the incompressible velocity fields $\mathbf{v}_{\pm} = \hat{\mathbf{z}} \times \nabla \varphi_{\pm}$. Such Lagrangian invariants and velocity fields generalize those of the model of Ref. [34].

We observe that the system admits also a further conserved quantity (which is not a Casimir invariant) corresponding to the generalized cross-helicity

$$\mathcal{H}_C = \frac{1}{2} \int N_e \left(1 - \frac{2\delta^2}{\beta_e} \Delta_{\perp}\right) A_{\parallel} d^3x. \quad (49)$$

This expression is similar to the invariant given by Eq. (33) of [14] where N_e identifies with the ion vorticity $\Delta_{\perp} \varphi$, and under the assumption of negligible parallel bulk velocity. It also rewrites

$$\mathcal{H}_C = \frac{1}{8} \int (G_+^2 - G_-^2) d^3x. \quad (50)$$

At large scales, where $N_e = \Delta_{\perp} \varphi$ and $A_e = A_{\parallel}$, one has $\mathcal{H}_C = -(1/2) \int \nabla A_{\parallel} \cdot \nabla \varphi d^3x = (1/2) \int \mathbf{B}_{\perp} \cdot \mathbf{u}_{\perp} d^3x$, which is the usual MHD cross-helicity, with $\mathbf{u}_{\perp} = \hat{\mathbf{z}} \times \nabla \varphi$ indicating the perpendicular velocity (corresponding, at leading order, to the $\mathbf{E} \times \mathbf{B}$ drift).

III. PHENOMENOLOGY OF CRITICALLY-BALANCED KAW TURBULENCE

In this section, we use the two-field gyrofluid model to phenomenologically characterize the energy and/or cross-helicity cascades which develop in strong KAW turbulence. The aim is to predict the transverse magnetic energy spectrum, commonly measured by satellite missions in the solar wind, together with the direct or inverse character of the cascades in the different spectral ranges delimited by the plasma characteristic scales.

A. Linear theory

At the linear level, using a hat to indicate Fourier transform of fields and Fourier symbols of operators, one has the phase velocity v_{ph} given by the dispersion relation

$$v_{ph}^2 \equiv \left(\frac{\omega}{k_z}\right)^2 = \frac{2}{\beta_e} \frac{k_{\perp}^2}{1 + \frac{2\delta^2 k_{\perp}^2}{\beta_e}} \frac{1 - \widehat{M}_1 + \widehat{M}_2}{\widehat{M}_2}, \quad (51)$$

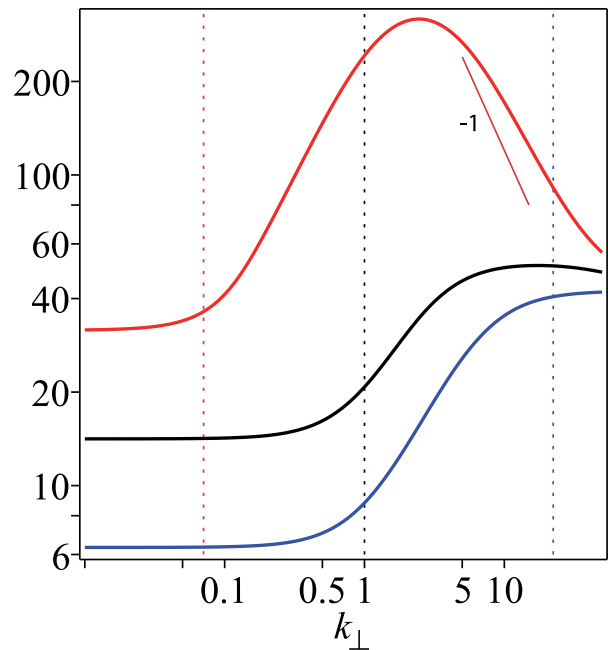


FIG. 1. Phase velocity of KAWs v_{ph} versus k_{\perp} for $\beta_e = 0.002$, $\tau = 100$ (red), $\beta_e = 0.01$, $\tau = 0.5$ (black) and $\beta_e = 0.05$, $\tau = 0.001$ (blue). The vertical dotted lines refer to the inverse ion Larmor radius ρ_i^{-1} for the three values of τ , with the same color code as for v_{ph} . Transition between MHD and sub-ion scales occurs at the smallest of the two scales ρ_i and ρ_s (which corresponds to $k_{\perp} = 1$). The orange straight line indicates the k_{\perp}^{-1} asymptotic behavior in the large τ limit.

where $1 - \widehat{M}_1 + \widehat{M}_2$ is strictly positive for all k_{\perp} . The associated eigenmodes obey

$$\widehat{A} = \frac{\beta_e}{2} v_{ph} \frac{\widehat{M}_2}{k_{\perp}^2} \widehat{\varphi}. \quad (52)$$

A graph of $v_{ph}(k_{\perp})$ is displayed in Fig. 1 for the cases $\beta_e = 0.002$, $\tau = 100$ (red), $\beta_e = 0.01$, $\tau = 0.5$ (black) and $\beta_e = 0.05$, $\tau = 0.001$ (blue). An important difference that appears at large τ , in addition to the shift of the dispersive zone towards smaller k_{\perp} (due to the fact that ρ_i is larger than ρ_s , here by a factor $\sqrt{200}$), is that at sub- d_e scales, v_{ph} does not stay constant but decreases as k_{\perp} increases (asymptotically like k_{\perp}^{-1} in the large τ limit), as in the full kinetic theory [16]. In the absence of the δ^2 term in L_3 , v_{ph} would be constant at small scales.

Interestingly, when assuming relation (52) in formula (44) for the energy \mathcal{H} , the sum of the first two terms of \mathcal{H} equals that of the last three ones.

The magnetic compressibility $\chi = |\widehat{B}_z|^2 / |\widehat{\mathbf{B}}_{\perp}|^2$ associated with the Alfvén eigenmode is then given by

$$\chi = \frac{2}{\beta_e} \left(1 + \frac{2\delta^2 k_{\perp}^2}{\beta_e}\right) \frac{\widehat{M}_1^2}{(1 - \widehat{M}_1 + \widehat{M}_2) \widehat{M}_2}. \quad (53)$$

Small τ limit ($\tau \sim \beta_e^{\frac{1}{2}}$): In this regime, $\widehat{M}_1 \sim \beta_e k_{\perp}^2 / 2$ and is thus negligible (and so is B_z). On the other hand,

$\widehat{M}_2 = (1 - \Gamma_0)/\tau + O(\delta^2) \approx k_\perp^2(1 - 3\tau k_\perp^2/4)$, leading to the dispersion relation

$$\left(\frac{\omega}{k_z}\right)^2 = \frac{2}{\beta_e} \frac{1}{1 + \frac{2\delta^2 k_\perp^2}{\beta_e}} \left(1 + k_\perp^2 + \frac{3}{4}\tau k_\perp^2\right). \quad (54)$$

B. Absolute equilibria

The invariants can be rewritten as

$$\mathcal{H} = \frac{1}{2} \int \left[(1 - \widehat{M}_1 + \widehat{M}_2) \widehat{M}_2 |\widehat{\varphi}|^2 + \frac{2k_\perp^2}{\beta_e} \left(1 + \frac{2\delta^2 k_\perp^2}{\beta_e}\right) |\widehat{A}_\parallel|^2 \right] d^2 k_\perp dk_z \quad (55)$$

$$\mathcal{H}_C = -\frac{1}{2} \int \left[\widehat{M}_2 \left(1 + \frac{2\delta^2 k_\perp^2}{\beta_e^2}\right) (\widehat{\varphi}_R \widehat{A}_{\parallel R} + \widehat{\varphi}_I \widehat{A}_{\parallel I}) \right] d^2 k_\perp dk_z \quad (56)$$

with $\widehat{\varphi} = \widehat{\varphi}_R + i\widehat{\varphi}_I$ and $\widehat{A}_\parallel = \widehat{A}_{\parallel R} + i\widehat{A}_{\parallel I}$, when separating real and imaginary parts.

Based on the existence of such quadratic invariants, a classical tool for predicting the direction of turbulent cascades is provided by the behavior of the spectral density of the corresponding invariants in the regime of absolute equilibrium. Albeit turbulence is intrinsically a non-equilibrium regime and a turbulent spectrum strongly differs from an equilibrium spectrum, the increasing or decreasing variation of the latter in the considered spectral range can be viewed as reflecting the direction of the turbulent transfer and thus the direct or inverse character of the cascade. An early application of this approach to incompressible MHD is found in Ref. [35].

In order to apply equilibrium statistical mechanics to the system consisting in a finite number of Fourier modes obtained by spectral truncation of the fields A_\parallel and φ governed by Eqs. (30) and (33), one first easily checks that the solution satisfies the Liouville's theorem conditions in the form

$$\sum_{\mathbf{k}} \frac{\partial}{\partial \widehat{\varphi}_{R\mathbf{k}}} \left(\frac{\partial \widehat{\varphi}_{R\mathbf{k}}}{\partial t} \right) + \frac{\partial}{\partial \widehat{\varphi}_{I\mathbf{k}}} \left(\frac{\partial \widehat{\varphi}_{I\mathbf{k}}}{\partial t} \right) = 0 \quad (57)$$

$$\sum_{\mathbf{k}} \frac{\partial}{\partial \widehat{A}_{\parallel R\mathbf{k}}} \left(\frac{\partial \widehat{A}_{\parallel R\mathbf{k}}}{\partial t} \right) + \frac{\partial}{\partial \widehat{A}_{\parallel I\mathbf{k}}} \left(\frac{\partial \widehat{A}_{\parallel I\mathbf{k}}}{\partial t} \right) = 0. \quad (58)$$

The density in phase space of the canonical equilibrium ensembles for the system (30)-(31), truncated in Fourier space, is given by $\rho = Z^{-1} \exp(-\lambda \mathcal{H} - \mu \mathcal{H}_C) = Z^{-1} \exp(-M_{ij} x^i x^j / 2)$, where Z is the partition function. The matrix M is defined as

$$\mathbf{M} = \begin{bmatrix} f & 0 & h & 0 \\ 0 & f & 0 & h \\ h & 0 & g & 0 \\ 0 & h & 0 & g \end{bmatrix},$$

where $f = \lambda(1 - \widehat{M}_1 + \widehat{M}_2) \widehat{M}_2$, $g = \lambda \frac{2k_\perp^2}{\beta_e} \left(1 + \frac{2\delta^2 k_\perp^2}{\beta_e}\right)$ and $h = \frac{\mu}{2} \widehat{M}_2 \left(1 + \frac{2\delta^2 k_\perp^2}{\beta_e^2}\right)$. Here, λ and μ denote numerical

constants prescribed by the values of the total energy and generalized cross-helicity. The symbols x^i , with $i=1, \dots, 4$, refer to $\widehat{\varphi}_R$, $\widehat{\varphi}_I$, $\widehat{A}_{\parallel R}$ and $\widehat{A}_{\parallel I}$. The matrix M should be positive definite, which corresponds to the conditions $f + g > 0$ and $fg - h^2 > 0$, aimed at ensuring positive eigenvalues. One easily checks that the former condition requires $\lambda > 0$. The inverse matrix easily writes

$$\mathbf{M}^{-1} = \frac{1}{\Delta} \begin{bmatrix} g & 0 & -h & 0 \\ 0 & g & 0 & -h \\ -h & 0 & f & 0 \\ 0 & -h & 0 & f \end{bmatrix},$$

with $\Delta = fg - h^2$. Without dissipation, the statistical equilibrium has an energy spectral density

$$E_k \sim \frac{1}{\lambda} 2\pi k_\perp (f E_k^\varphi + g E_k^{A_\parallel}) \quad (59)$$

and a generalized cross-helicity spectral density

$$H_k \sim \frac{1}{\mu} 4\pi k_\perp h E_k^{\varphi A_\parallel}, \quad (60)$$

where $E_k^\varphi = g/\Delta$, $E_k^{A_\parallel} = f/\Delta$ and $E_k^{\varphi A_\parallel} = -h/\Delta$.

The cascade directions are forward or backward, depending on whether the absolute equilibrium spectra are respectively growing or decreasing in the wavenumber ranges of interest. The energy spectrum rewrites

$$E_k \sim \frac{4\pi}{\lambda} \frac{k_\perp}{1 - \frac{\mu^2}{4\lambda^2} \frac{1}{v_{ph}^2}}. \quad (61)$$

Positivity condition prescribes constraints on the wavenumber domain where this formula applies. The condition $|\mu|/\lambda \lesssim 2 \min(v_{ph})$ (where $\min(v_{ph}) = \sqrt{8/\beta_e}$ for small τ but is smaller for larger values of τ), ensures that the energy spectrum is defined for all wavenumbers. For larger values of $|\mu|/\lambda$, there is a lower bound in k_\perp and possibly also an upper bound, for which $E_k > 0$. As v_{ph} is bounded from above, it might happen that the energy is never positive. A more detailed study would require an explicit calculation of the constant λ and μ . Nevertheless, in all the cases where it is defined, the energy is found to be a growing function of k_\perp (except possibly near the lower k_\perp bound where it has a singular behavior), whatever the values of β_e and τ , indicating a forward cascade. The generalized cross-helicity spectrum, on the other hand, rewrites

$$H_k \sim -\frac{4\pi}{\mu} \frac{k_\perp}{\frac{4\lambda^2}{\mu^2} v_{ph}^2 - 1}. \quad (62)$$

We thus have the relation $H_k = -\mu E_k / (4\lambda v_{ph}^2)$. In the same wavenumber ranges where the energy is positive, its absolute value is a growing quantity both at MHD and sub- d_e scales. However, in the intermediate (sub- ρ_s or sub- ρ_i) range, where $\omega/k_z \sim k_\perp$, it is a decreasing

function of k_\perp , indicating an inverse cascade. Note that when the $-7/3$ power law of the turbulent transverse magnetic energy spectrum is not well developed (see next Section), the range of the generalized cross-helicity inverse cascade is also very limited. Similar results showing an inverse (or direct) cross-helicity cascade in the Hall (respectively sub-electronic) range are obtained in Ref. [36] based on absolute equilibrium arguments in extended MHD (XMHD).

C. Turbulent spectra

1. Energy cascade

We here discuss the turbulent state in the presence of a small amount of dissipation at small scales (leading to a finite flux of energy), focusing on the case of a critically balanced KAW cascade (with equal amount of positively and negatively propagating waves). Following the discussion of Section 7 in Ref. [16], the magnetic spectrum is easily obtained by imposing a constant energy flux, estimated by the ratio of the spectral energy density at a given scale by the nonlinear transfer time at this scale. In the strong wave (critically-balanced) turbulence regime, this energy transfer time reduces to the nonlinear timescale. Let us mention at this point that the estimates of the nonlinear times and the relation between the fields are identical to those of the purely nonlinear regime that occurs for example in two dimensions. To estimate these quantities, it is first necessary to relate the Fourier components of the electric and magnetic potentials. This is achieved by assuming the linear relationship, characteristic of Alfvén modes, provided by Eq. (52). After inserting this relation into the energy \mathcal{H} , one finds that the total 3D spectral energy density reads

$$\mathcal{E}_k^{3D} = \frac{2}{\beta_e} k_\perp^2 \left(1 + \frac{2\delta^2 k_\perp^2}{\beta_e} \right) |\widehat{A}_k|^2. \quad (63)$$

Due to the quasi-2D character of the dynamics, it is convenient to deal with the 2D energy spectrum

$$\mathcal{E}_k^{2D} = \frac{2}{\beta_e} k_\perp^2 \left(1 + \frac{2\delta^2 k_\perp^2}{\beta_e} \right) |\widehat{A}_{k_\perp}|^2, \quad (64)$$

where we used the notation

$$|\widehat{A}_{k_\perp}|^2 = \int |\widehat{A}_k|^2 dk_z \quad (65)$$

and assume statistical isotropy in the transverse plane. Similar definitions are used for the other relevant fields, namely the electrostatic potential φ and the transverse magnetic field \mathbf{B}_\perp .

The nonlinear timescale is estimated from Eq. (31) which, after discarding the B_z terms (smaller by a factor β_e) and the ∂_z terms, can be rewritten as

$$\partial_t A_e + [\varphi, A_e] - [A_\parallel, M_2 \varphi] = 0. \quad (66)$$

Assuming locality of the nonlinear interactions in Fourier space, the typical frequencies at wavenumber k_\perp associated with the two nonlinear terms of the above equation take the form $\tau_{NL1}^{-1}(k_\perp) \sim k_\perp^2 |\widehat{\varphi}_{k_\perp}|$ and $\tau_{NL2}^{-1}(k_\perp) \sim k_\perp^2 \widehat{M}_2 |\widehat{\varphi}_{k_\perp}| / (1 + 2\delta^2 k_\perp^2 / \beta_e)$ respectively. As usual in the turbulence statistical theory (see e.g. Ref. [37]), the global nonlinear frequency of the system can be estimated by a linear combination of these two frequencies. Taking equal weights leads to the estimate

$$\tau_{NL}^{-1}(k_\perp) \sim \frac{2}{\beta_e} k_\perp^4 \left(1 + \frac{\widehat{M}_2}{1 + \frac{2\delta^2 k_\perp^2}{\beta_e}} \right) \frac{1}{\widehat{M}_2 v_{ph}} |\widehat{A}_{k_\perp}|. \quad (67)$$

In two-dimensions, when assuming isotropy, the transverse magnetic energy spectral density $|\widehat{B}_\perp(k_\perp)|^2 \sim k_\perp^2 |\widehat{A}_{k_\perp}|^2$ is related to the transverse magnetic energy spectrum by $E_{B_\perp}(k_\perp) \sim k_\perp^{-1} |\widehat{B}_\perp(k_\perp)|^2$, the energy flux ε writes

$$\varepsilon \sim \frac{4}{\beta_e^2} \left(1 + \frac{2\delta^2 k_\perp^2}{\beta_e} + \widehat{M}_2 \right) \frac{1}{\widehat{M}_2 v_{ph}} k_\perp^3 |\widehat{B}_\perp(k_\perp)|^3, \quad (68)$$

and thus, assuming a constant energy flux, one gets

$$E_{B_\perp}(k_\perp) \sim \varepsilon^{2/3} \beta_e^{4/3} k_\perp^{-3} \left(\frac{v_{ph} \widehat{M}_2}{1 + \frac{2\delta^2 k_\perp^2}{\beta_e} + \widehat{M}_2} \right)^{2/3}. \quad (69)$$

All the regimes of KAW energy cascade can be recovered from Eq. (69).

- *MHD range*

At scales large compared to ρ_s and ρ_i , one has $v_{ph} \sim (2/\beta_e)^{1/2}$, $\widehat{M}_2 = k_\perp^2$ and $k \ll 1$. One thus immediately finds $E_B(k) \sim \varepsilon^{2/3} k_\perp^{-5/3}$.

- *Sub- ρ_i range*

When $\sqrt{\beta_e}/2/\delta \geq k_\perp \gtrsim (2\tau)^{-1/2}$ and $\tau \geq 1$ (i.e. for scales smaller than the ion gyroradius (assumed larger than ρ_s), for which $\Gamma_0 \approx 0$ and $\Gamma_1 \approx 0$, and large enough for electron inertia to be negligible), one has $\widehat{M}_2 \sim 1/\tau + \beta_e(1+\tau)/(2\tau) \sim \text{constant}$ and $v_{ph} \sim k_\perp$, so that $E_B(k) \sim \varepsilon^{2/3} k_\perp^{-7/3}$.

- *Sub- ρ_s range*

When, on the other hand, $\tau \leq 1$, for scales intermediate between ρ_s and d_e , characterized by $k_\perp \gg 1$ and $2\delta^2 k_\perp^2 / \beta_e \ll 1$, one finds $\widehat{M}_2 \sim k_\perp^2$ and $v_{ph} \sim (2/\beta_e)^{1/2} k_\perp$, so that again $E_{B_\perp}(k_\perp) \sim \varepsilon^{2/3} k_\perp^{-7/3}$. It is however to be noted that in this case, the smallest nonlinear time scale is not the stretching time τ_{NL1} but rather τ_{NL2} , associated with the electron pressure term in Ohm's law.

- *Sub- d_e range*

When β_e is small enough, it is possible to observe a third power law at scales smaller than the electron inertial length (but still larger than the electron Larmor radius).

– When $\tau \ll 1$, the $-7/3$ power-law zone is almost inexistent. It is replaced by a smooth transition between the $-5/3$ power-law and a steeper zone where $v_{ph} \sim \text{cst}$, $\widehat{M}_2 \sim k_{\perp}^2$ and thus where $E_B(k) \sim \varepsilon^{2/3} k_{\perp}^{-3}$.

– If τ is taken larger than unity, $v_{ph} \sim k_{\perp}^{-1}$ and $\widehat{M}_2 \sim k_{\perp}^2$, leading to $E_{B_{\perp}}(k_{\perp}) \sim \varepsilon^{2/3} k_{\perp}^{-11/3}$.

– Note that for a small range of parameters where $\beta_e \ll 1$ and $\tau = O(1)$, a regime where one can have $v_{ph} \sim \text{constant}$ and $\widehat{M}_2 \sim \text{constant}$, one recovers a spectrum of the form $E_{B_{\perp}}(k_{\perp}) \sim \varepsilon^{2/3} k_{\perp}^{-13/3}$, as mentioned in Ref. [16].

2. Generalized cross-helicity cascade

We here derive the expected transverse magnetic energy spectrum associated with a generalized cross-helicity cascade. Proceeding as in the case of the energy cascade, we first write the 3D spectral density (taken positive)

$$\mathcal{H}_k^{3D} = \frac{1}{\beta_e v_{ph}} \left(1 + \frac{2\delta^2 k^2}{\beta_e} \right) k_{\perp}^2 |\widehat{A}_{\mathbf{k}}|^2. \quad (70)$$

Keeping the same estimate for the transfer time, and assuming a constant generalized cross-helicity flux rate η , we obtain the magnetic spectrum in the generalized cross-helicity cascade

$$E_{B_{\perp}}(k_{\perp}) \sim \eta^{2/3} \beta_e^{4/3} k_{\perp}^{-3} \left(\frac{v_{ph}^2 \widehat{M}_2}{1 + \frac{2\delta^2 k^2}{\beta_e} + \widehat{M}_2} \right)^{2/3}. \quad (71)$$

Going through the same estimates in the various wavenumber domains as for the energy cascade, we now see that the magnetic spectrum in the generalized cross-helicity cascade obeys a $-5/3$ power law from the MHD range to the electron scale. At scales smaller than d_e , we differently find that for $\tau \ll 1$ the spectrum is proportional to k_{\perp}^{-3} , while it is otherwise proportional to $k_{\perp}^{-13/3}$. It is of interest to remark that this latter scaling is somewhat similar to the M_{H+} spectrum of Ref. [38] associated to the magnetic spectrum of the magnetosonic cyclotron branch in the so-called H-generalized helicity cascade computed on exact solutions of an extended MHD model (with the caveat that in Ref. [38] a singularity appears at the d_e scale).

Examples of transverse spectra are displayed for the parameters $\beta_e = 0.002$, $\tau = 100$ (Fig. 2), $\beta_e = 0.01$, $\tau = 0.5$ (Fig. 3) and $\beta_e = 0.05$, $\tau = 0.001$ (Fig. 4). They concern both the absolute equilibria (long dashed lines) energy (black) and generalized cross-helicity (red) and turbulent magnetic spectra (solid lines) associated with the energy (black) and generalized cross-helicity cascades (red). The generalized cross-helicity inverse cascade associated with the decreasing absolute equilibrium spectrum in sub-ion range, is conspicuous in the case of large τ , but less pronounced for τ of order unity.

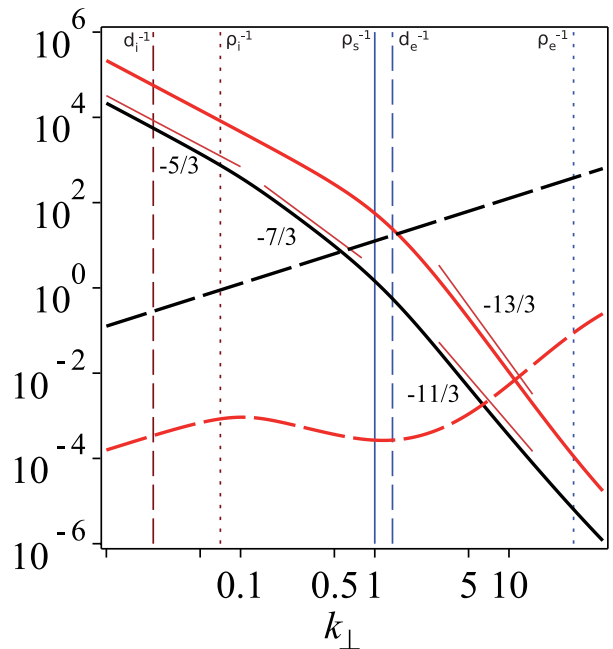


FIG. 2. Turbulent magnetic spectra (solid lines) in energy (black) and generalized cross-helicity (red) cascades, together with absolute equilibrium energy (black long dashed lines) and generalized cross-helicity (red long dashed lines) spectra for $\beta_e = 0.002$, $\tau = 100$. Straight orange lines refer to the slopes of the various power-law inertial ranges: $-5/3$ in the MHD range, $-7/3$ in the sub-ion Larmor radius range and $-11/3$ (for the energy cascade) or $-13/3$ (for the cross-helicity cascade) in the sub- d_e range. The blue solid vertical line refers to ρ_s^{-1} , the brown and blue long-dashed (respectively dotted) vertical lines to the inverse ion and electron inertial lengths (respectively Larmor radii) d_i^{-1} and d_e^{-1} (respectively ρ_i^{-1} and ρ_e^{-1}).

IV. CONCLUSION

In this paper, a new reduced model, given by Eqs. (37)-(38), has been derived for low- β_e plasmas. It is a two-field gyrofluid model, valid for any τ , which retains both electron inertia and B_z fluctuations, in addition to ion FLR contributions. It is used to present a comprehensive phenomenological description of the Alfvén wave magnetic energy spectrum from the MHD scales to scales smaller than d_e (while larger than ρ_e). Assuming the existence of energy or generalized cross-helicity cascades leads to the prediction of the magnetic energy spectrum when neglecting possible intermittency effects originating from the presence of coherent structures. The magnetic energy spectra observed in the solar wind at the sub-ion scales are usually steeper than the predicted $-7/3$ exponent. In addition they turn out to be non-universal, covering a range $(-3.5, -2.1)$, with a most probable value close to -2.8 [6]. Intermittency [11], Landau damping [39] and possible other effects not included in the present model could contribute to the observed behavior.

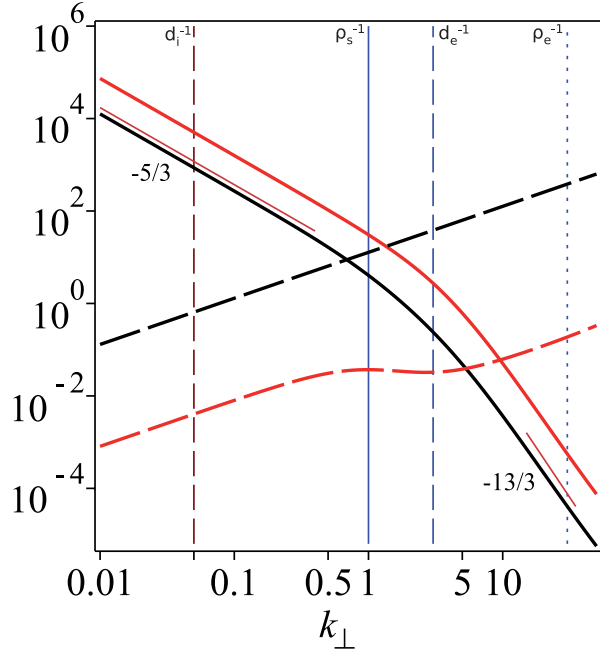


FIG. 3. Same as for Fig. 2 for $\beta_e = 0.01$, $\tau = 0.5$. No sub-ion power-law range is visible. Both for the energy and cross-helicity cascades, the magnetic spectrum displays a $-13/3$ sub- d_e power-law range.

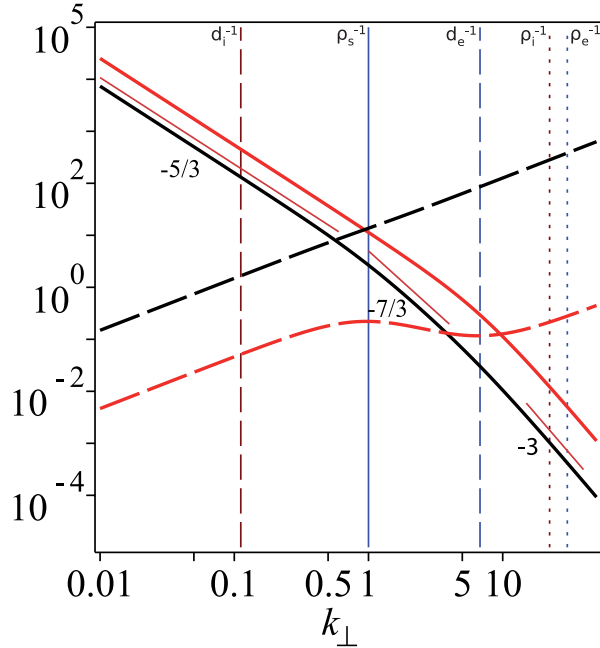


FIG. 4. Same as for Fig. 2 for $\beta_e = 0.05$, $\tau = 0.001$. A $-7/3$ power-law turbulent magnetic spectrum in the energy cascade is visible for $k_\perp > 1$, while, both for the energy and cross-helicity cascades, the magnetic spectrum displays a -3 sub- d_e power-law range.

The existence of the cascades needs to be confirmed by numerical simulations of the gyrofluid equations supplemented by dissipation and energy and/or cross-helicity injection. In particular, the inverse cross-helicity cascade is expected to occur only when the system is driven at a scale close to d_e , in a way that mostly injects cross-helicity rather than energy. In fact, Eq. (50) shows that a non-zero cross-helicity corresponds to an imbalanced regime where either G_+ or G_- dominates. It is interesting to note that the evidence of an inverse cross-helicity cascade in numerical simulations of imbalanced EMHD turbulence was reported in Refs. [40, 41]. Analytic considerations on the role of cross-helicity in weak reduced EMHD turbulence can also be found in Ref. [42]. An imbalanced energy injection could possibly originate from magnetic reconnection that takes place at the electronic scales. This scenario was recently considered in Ref. [43] on the basis of 2D hybrid PIC and Vlasov simulations where the development of a sub-ion magnetic energy spectrum occurs in relation with the reconnection instability, before the direct energy cascade reaches this scale.

In the framework of the two-field gyrofluid model, the transition scale between the $k_\perp^{-5/3}$ and the $k_\perp^{-7/3}$ ranges occurs at the largest of the two scales ρ_i and ρ_s . When τ is small, this is easily shown, as can be found for example in appendix E.4 of Ref. [10]. Differently for $\tau \sim 1$ and small β_e , a spectral transition is observed to take place at scale d_i , both in the solar wind [9] and in hybrid-PIC simulations [22]. The question arises whether a similar transition could also be observed in numerical simulations of reduced models, induced by the presence of current sheets and the occurrence of reconnection processes, or if more physical effects have to be taken into account.

Note that while the magnetic energy spectrum displays a $k_\perp^{-7/3}$ below the transition scale given by the largest of the characteristic scales ρ_i and ρ_s , when β_e is small, the perpendicular electric field spectrum behaves in this range like $k_\perp^{-1/3}$ when the transition takes place at ρ_i and like $k_\perp^{-13/3}$ when it occurs at ρ_e .

The two-field gyrofluid model derived in this paper could be extended to account for electron Landau damping, a crucial ingredient at small β_e , with either a Landau-fluid formulation, as suggested in Ref. [16], or with the coupling with a drift-kinetic equation. In the latter case, it could provide an interesting generalization of the model presented in Ref. [44], by taking into account the parallel magnetic field fluctuations and thus permitting larger values of β_e .

At sub- d_e scales, a new regime is uncovered in the case of cold ions (small τ), where the magnetic energy density scales like k_\perp^{-3} . Compressibility here plays a central role, which explains the difference with the cases $\tau \sim 1$ where the spectrum scales like $k_\perp^{-13/3}$ or $\tau \gg 1$ (a quasi-incompressible limit) where it scales like $k_\perp^{-11/3}$. Scales smaller than ρ_e are not considered in this paper, as they require a full description of the electron FLR effects. In

this regime, the spectrum is observed to be even steeper [45], possibly associated with a phase-space entropy cascade [10].

Appendix A: Parent gyrofluid model

We consider the gyrofluid equations for the evolution of the dimensional gyrocenter moments $\tilde{N}_{e,i}$, $\tilde{U}_{e,i}$, $\tilde{P}_{\parallel e,i}$, $\tilde{P}_{\perp e,i}$, $\tilde{Q}_{\parallel e,i}$, $\tilde{Q}_{\perp e,i}$, $\tilde{R}_{\parallel \perp e,i}$ and $\tilde{R}_{\perp \perp e,i}$ corresponding to the fluctuations of gyrocenter density, parallel velocity, parallel and perpendicular pressure, parallel and perpendicular heat flux, and of the parallel/parallel and parallel/perpendicular components of the energy weighted pressure tensor respectively, with the subscript e and i referring to electrons and ions. Similarly to what is done in Ref. [25], we define the following non-dimensional quantities :

$$\begin{aligned}
t &= \Omega_i \tilde{t}, & x &= \frac{\tilde{x}}{\rho_s}, & y &= \frac{\tilde{y}}{\rho_s}, & z &= \frac{\tilde{z}}{\rho_s}, \\
k_{\perp} &= \tilde{k}_{\perp} \rho_s, & k_z &= \tilde{k}_z \rho_s, \\
N_{\alpha} &= \frac{\tilde{N}_{\alpha}}{n_0}, & U_{\alpha} &= \frac{\tilde{U}_{\alpha}}{c_s}, & P_{\parallel \alpha} &= \frac{\tilde{P}_{\parallel \alpha}}{n_0 T_{\alpha}}, & P_{\perp \alpha} &= \frac{\tilde{P}_{\perp \alpha}}{n_0 T_{\alpha}}, \\
Q_{\parallel \alpha} &= \frac{\tilde{Q}_{\parallel \alpha}}{n_0 T_{\alpha} c_s}, & Q_{\perp \alpha} &= \frac{\tilde{Q}_{\perp \alpha}}{n_0 T_{\alpha} c_s}, \\
R_{x_{\alpha}} &= m_{\alpha} \frac{\tilde{R}_{x_{\alpha}}}{n_0 T_{\alpha}^2}, & R_{\perp \alpha}^{(\perp)} &= m_{\alpha} \frac{\tilde{R}_{\perp \alpha}^{(\perp)}}{n_0 T_{\alpha}^2}, \\
\varphi &= \frac{e \tilde{\varphi}}{T_e}, & A_{\parallel} &= \frac{\tilde{A}_{\parallel}}{B_0 \rho_s}, & B_z &= \frac{\tilde{B}_z}{B_0}.
\end{aligned} \tag{A1}$$

The equations read

$$\frac{\partial N_e}{\partial t} + [e^{\delta^2 \Delta_s} \varphi, N_e] + \delta^2 [\Delta_s e^{\delta^2 \Delta_s} \varphi, P_{\perp e} - N_e] \tag{A2}$$

$$\begin{aligned}
&- [e^{\delta^2 \Delta_s} A_{\parallel}, U_e] - [e^{\delta^2 \Delta_s} B_z, P_{\perp e}] \\
&- \delta^2 [\Delta_s e^{\delta^2 \Delta_s} B_z, P_{\perp e} - N_e] + \frac{\partial U_e}{\partial z} = 0, \tag{A3}
\end{aligned}$$

$$\begin{aligned}
&\frac{\partial}{\partial t} \left(\delta^2 U_e - e^{\delta^2 \Delta_s} A_{\parallel} \right) + \delta^2 [e^{\delta^2 \Delta_s} \varphi, U_e] - [e^{\delta^2 \Delta_s} A_{\parallel}, P_{\parallel e}] \\
&- \delta^2 [\Delta_s e^{\delta^2 \Delta_s} A_{\parallel}, P_{\perp e} - N_e] - \delta^2 [e^{\delta^2 \Delta_s} B_z, U_e] \tag{A4}
\end{aligned}$$

$$\begin{aligned}
&- \delta^2 [B_z, Q_{\perp e}] - \bar{\Gamma}_0 (\delta^2 \Delta_s^{\varphi}, \delta^2 \Delta_s^A) [\varphi, A_{\parallel}] \\
&+ (\bar{\Gamma}_0 (\delta^2 \Delta_s^B, \delta^2 \Delta_s^A) + \delta^2 \Delta_s \bar{\Gamma}_1 (\delta^2 \Delta_s^B, \delta^2 \Delta_s^A)) [B_z, A_{\parallel}] \\
&+ \frac{\partial}{\partial z} \left(P_{\parallel e} - e^{\delta^2 \Delta_s} \varphi + e^{\delta^2 \Delta_s} B_z \right) = 0, \tag{A5}
\end{aligned}$$

$$\begin{aligned}
&\frac{\partial P_{\parallel e}}{\partial t} + [e^{\delta^2 \Delta_s} \varphi, P_{\parallel e}] + \delta^2 [\Delta_s e^{\delta^2 \Delta_s} \varphi, P_{\perp e} - N_e] - [A_{\parallel}, Q_{\parallel e}] \\
&- 3 [e^{\delta^2 \Delta_s} A_{\parallel}, U_e] - [e^{\delta^2 \Delta_s} B_z, P_{\parallel e} + P_{\perp e} - N_e] \\
&- \delta^2 [\Delta_s e^{\delta^2 \Delta_s} B_z, P_{\perp e} - N_e] - [B_z, R_{\parallel \perp e}] \\
&+ \frac{\partial}{\partial z} (Q_{\parallel e} + 3U_e) = 0, \tag{A6}
\end{aligned}$$

$$\begin{aligned}
&\frac{\partial P_{\perp e}}{\partial t} + [(1 + \delta^2 \Delta_s) e^{\delta^2 \Delta_s} \varphi, P_{\perp e}] \\
&+ \delta^2 [\Delta_s (2 + \delta^2 \Delta_s) e^{\delta^2 \Delta_s} \varphi, P_{\perp e} - N_e] - [e^{\delta^2 \Delta_s} A_{\parallel}, U_e] \\
&- [A_{\parallel}, Q_{\perp e}] - [(2 + \delta^2 \Delta_s) e^{\delta^2 \Delta_s} B_z, 2P_{\perp e} - N_e] \\
&- \delta^2 [\Delta_s (3 + \delta^2 \Delta_s) e^{\delta^2 \Delta_s} B_z, P_{\perp e} - N_e] \\
&- 2 [B_z, R_{\perp \perp e}] + \frac{\partial}{\partial z} (U_e + Q_{\perp e}) = 0, \tag{A7}
\end{aligned}$$

$$\begin{aligned}
&\frac{\partial N_i}{\partial t} + [e^{\tau \Delta_s} \varphi, N_i] + \tau [\Delta_s e^{\tau \Delta_s} \varphi, P_{\perp i} - N_i] - [e^{\tau \Delta_s} A_{\parallel}, U_i] \\
&+ \tau [e^{\tau \Delta_s} B_z, P_{\perp i}] + \tau^2 [\Delta_s e^{\tau \Delta_s} B_z, P_{\perp i} - N_i] + \frac{\partial U_i}{\partial z} = 0, \tag{A8}
\end{aligned}$$

$$\begin{aligned}
&\frac{\partial}{\partial t} (U_i + e^{\tau \Delta_s} A_{\parallel}) + [e^{\tau \Delta_s} \varphi, U_i] - \tau [e^{\tau \Delta_s} A_{\parallel}, P_{\parallel i}] \\
&- \tau^2 [\Delta_s e^{\tau \Delta_s} A_{\parallel}, P_{\perp i} - N_i] + \tau [e^{\tau \Delta_s} B_z, U_i] + \tau [B_z, Q_{\perp i}] \\
&+ \bar{\Gamma}_0 (\tau \Delta_s^{\varphi}, \tau \Delta_s^A) [\varphi, A_{\parallel}] \\
&+ \tau (\bar{\Gamma}_0 (\tau \Delta_s^B, \tau \Delta_s^A) + \tau \Delta_s \bar{\Gamma}_1 (\tau \Delta_s^B, \tau \Delta_s^A)) [B_z, A_{\parallel}] \\
&+ \frac{\partial}{\partial z} (\tau P_{\parallel i} + e^{\tau \Delta_s} \varphi + \tau e^{\tau \Delta_s} B_z) = 0, \tag{A9}
\end{aligned}$$

$$\begin{aligned}
&\frac{\partial P_{\parallel i}}{\partial t} + [e^{\tau \Delta_s} \varphi, P_{\parallel i}] + \tau [\Delta_s e^{\tau \Delta_s} \varphi, P_{\perp i} - N_i] - [A_{\parallel}, Q_{\parallel i}] \\
&- 3 [e^{\tau \Delta_s} A_{\parallel}, U_i] + \tau [e^{\tau \Delta_s} B_z, P_{\parallel i} + P_{\perp i} - N_i] \\
&+ \tau^2 [\Delta_s e^{\tau \Delta_s} B_z, P_{\perp i} - N_i] + \tau [B_z, R_{\parallel \perp i}] \\
&+ \frac{\partial}{\partial z} (Q_{\parallel i} + 3U_i) = 0, \tag{A10}
\end{aligned}$$

$$\begin{aligned}
&\frac{\partial P_{\perp i}}{\partial t} + [(1 + \tau \Delta_s) e^{\tau \Delta_s} \varphi, P_{\perp i}] \\
&+ \tau [\Delta_s (2 + \tau \Delta_s) e^{\tau \Delta_s} \varphi, P_{\perp i} - N_i] \\
&- [e^{\tau \Delta_s} A_{\parallel}, U_i] - [A_{\parallel}, Q_{\perp i}] \\
&+ \tau [(2 + \tau \Delta_s) e^{\tau \Delta_s} B_z, 2P_{\perp i} - N_i] \\
&+ \tau^2 [\Delta_s (3 + \tau \Delta_s) e^{\tau \Delta_s} B_z, P_{\perp i} - N_i] \\
&+ 2\tau [B_z, R_{\perp \perp i}] + \frac{\partial}{\partial z} (U_i + Q_{\perp i}) = 0, \tag{A11}
\end{aligned}$$

together with Poisson's equations and parallel and perpendicular Ampère's laws, which respectively read

$$\begin{aligned}
&\frac{v_A^2}{c^2} \Delta_{\perp} \varphi = e^{\delta^2 \Delta_s} N_e + \delta^2 \Delta_s e^{\delta^2 \Delta_s} (P_{\perp e} - N_e) \\
&- (I_0 (2\delta^2 \Delta_s) e^{2\delta^2 \Delta_s} - 1) \varphi \\
&+ (I_0 (2\delta^2 \Delta_s) - I_1 (2\delta^2 \Delta_s)) e^{2\delta^2 \Delta_s} B_z \\
&- e^{\tau \Delta_s} N_i - \tau \Delta_s e^{\tau \Delta_s} (P_{\perp i} - N_i) - (I_0 (2\tau \Delta_s) e^{2\tau \Delta_s} - 1) \frac{\varphi}{\tau} \\
&- (I_0 (2\tau \Delta_s) - I_1 (2\tau \Delta_s)) e^{2\tau \Delta_s} B_z, \tag{A12}
\end{aligned}$$

$$\Delta_{\perp} A_{\parallel} = \frac{\beta_e}{2} (e^{\delta^2 \Delta_s} U_e - e^{\tau \Delta_s} U_i), \tag{A13}$$

and

$$\begin{aligned}
B_z = & -\frac{\beta_e}{2} \left(e^{\delta^2 \Delta_s} P_{\perp e} + \delta^2 \Delta_s e^{\delta^2 \Delta_s} (P_{\perp e} - N_e) \right. \\
& - (I_0(2\delta^2 \Delta_s) - I_1(2\delta^2 \Delta_s)) e^{2\delta^2 \Delta_s} \varphi \\
& + 2(I_0(2\delta^2 \Delta_s) - I_1(2\delta^2 \Delta_s)) e^{2\delta^2 \Delta_s} B_z \\
& + \tau e^{\tau \Delta_s} P_{\perp i} + \tau^2 \Delta_s e^{\tau \Delta_s} (P_{\perp i} - N_i) \\
& + (I_0(2\tau \Delta_s) - I_1(2\tau \Delta_s)) e^{2\tau \Delta_s} \varphi \\
& \left. + 2\tau (I_0(2\tau \Delta_s) - I_1(2\tau \Delta_s)) e^{2\tau \Delta_s} B_z \right). \tag{A14}
\end{aligned}$$

The operators $\bar{\Gamma}_0$ and $\bar{\Gamma}_1$ and Δ_s are defined as $\bar{\Gamma}_0(z, z') = I_0(z z') \exp(z + z')$, $\bar{\Gamma}_1(z, z') = I_1(z z') \exp(z + z')$ and $\Delta_s = \frac{1}{2} \Delta_{\perp}$, with I_0 and I_1 indicating the modified Bessel function of the first kind of order zero and one, respectively.

The set of gyrofluid equations (A3)-(A14) was derived in Ref. [20], although with a different normalization and with the combination $I_0 + I_1$ instead of $I_0 - I_1$ in Eqs. (A12) and (A14). In Eqs. (A3)-(A14), we corrected a few typographical errors that were present in the corresponding equations of Ref. [25] (where they had no effect in the considered asymptotics).

Appendix B: Derivation of the two-field evolution equations from the electron drift-kinetic equation via a Hamiltonian closure

In this Section we show that the evolution equations (30) and (31) can be obtained from an electron drift-kinetic equation by applying a closure relation which guarantees a Hamiltonian structure in the resulting model.

Because the application of the scalings I and II of Sec. IIB eventually leads to neglecting electron FLR corrections in the evolution equations, in this alternative derivation we start from an electron drift-kinetic equation, which already assumes $k_{\perp} \rho_e \ll 1$ and thus neglects electron FLR corrections. The drift-kinetic equation under consideration, corresponding to Eq. (B1) below, can be obtained, for instance, from Ref. [20], upon neglecting electron finite Larmor radius corrections and background inhomogeneities. On the other hand, we assume that electron and ion FLR corrections are included in the equations relating electromagnetic perturbations to the perturbations of the gyrofluid moments. Therefore, we assume Eqs. (28), (32) and (33) to be valid.

We consider, as starting point, the following electron drift-kinetic equation, in the so-called δf approximation, in dimensional form (we indicate with a tilde dimensional quantities and, in particular, $[f, g] = \partial_{\tilde{x}} f \partial_{\tilde{y}} g - \partial_{\tilde{y}} f \partial_{\tilde{x}} g$ indicates the canonical Poisson bracket between two functions f and g , in dimensional form) :

$$\frac{\partial \tilde{g}_e}{\partial \tilde{t}} + \frac{c}{B_0} \left[\tilde{\varphi} - \frac{\tilde{v}}{c} \tilde{A}_{\parallel} - \frac{\tilde{\mu}_e}{e} \tilde{B}_z, \tilde{g}_e \right]$$

$$+ \tilde{v} \frac{\partial}{\partial \tilde{z}} \left(\tilde{g}_e - \frac{e}{T_{0e}} \left(\tilde{\varphi} - \frac{\tilde{v}}{c} \tilde{A}_{\parallel} - \frac{\tilde{\mu}_e}{e} \tilde{B}_z \right) \tilde{\mathcal{F}}_{eqe} \right) = 0. \tag{B1}$$

In Eq. (B1) $\tilde{g}_e = \tilde{f}_e - (e/T_{0e})(\tilde{v}/c)\tilde{\mathcal{F}}_{eqe}\tilde{A}_{\parallel}$, where \tilde{f}_e is the perturbation of the electron gyrocenter distribution function around a homogeneous equilibrium Maxwellian distribution

$$\tilde{\mathcal{F}}_{eqe}(\tilde{v}, \tilde{\mu}_e) = n_0 \left(\frac{m_e}{2\pi T_{0e}} \right)^{3/2} \exp \left(-\frac{m_e \tilde{v}^2}{2T_{0e}} - \frac{\tilde{\mu}_e B_0}{T_{0e}} \right), \tag{B2}$$

where \tilde{v} is the velocity coordinate along the guide field and $\tilde{\mu}_e$ is the electron magnetic moment. Upon introducing the electron gyrocenter density and parallel velocity fluctuations as

$$\tilde{N}_e = \int d\tilde{\mathcal{W}} \tilde{f}_e, \quad \tilde{U}_e = \frac{1}{n_0} \int d\tilde{\mathcal{W}} \tilde{v} \tilde{f}_e, \tag{B3}$$

where $d\tilde{\mathcal{W}} = (2\pi B_0/m_e)d\tilde{\mu}_e d\tilde{v}$ is the volume element in velocity space, Eq. (B1) is complemented by the following relations:

$$\begin{aligned}
\frac{e\tilde{\varphi}}{T_{0e}} = & -M_2^{-1} \frac{\tilde{N}_e}{n_0}, \quad \tilde{\Delta}_{\perp} \frac{\tilde{A}_{\parallel}}{B_0 \rho_s} = \frac{\beta_e}{2} \frac{\tilde{U}_e}{c_s}, \\
\frac{\tilde{B}_z}{B_0} = & M_1 \frac{e\tilde{\varphi}}{T_{0e}}. \tag{B4}
\end{aligned}$$

Equations (B4) are those introduced in Sec. IID in dimensional form. By means of the relations (B3), from Eqs. (B4) one can express perturbations of electromagnetic potentials as well as of the parallel magnetic field in terms of the perturbation of the distribution function \tilde{f}_e (and thus in terms of \tilde{g}_e). The system (B1)-(B4) possesses a noncanonical Hamiltonian structure with Hamiltonian

$$\mathcal{H} = \frac{1}{2} \int d^3 \tilde{x} d\tilde{\mathcal{W}} \left(T_{0e} \frac{\tilde{g}_e^2}{\tilde{\mathcal{F}}_{eqe}} - e \left(\tilde{\varphi} - \frac{\tilde{v}}{c} \tilde{A}_{\parallel} - \frac{\tilde{\mu}_e}{e} \tilde{B}_z \right) \tilde{g}_e \right) \tag{B5}$$

and Poisson bracket

$$\{F, G\} = \int d^3 \tilde{x} d\tilde{\mathcal{W}} \left(\frac{c}{e B_0} \tilde{g}_e [F_{\tilde{g}_e}, G_{\tilde{g}_e}] - \tilde{v} \frac{\tilde{\mathcal{F}}_{eqe}}{T_{0e}} F_{\tilde{g}_e} \frac{\partial}{\partial \tilde{z}} G_{\tilde{g}_e} \right). \tag{B6}$$

From Eq. (B1) one can obtain the following two equations governing the evolution of the moments of order zero and one, with respect to the coordinate \tilde{v} of the generalized perturbed distribution function \tilde{g}_e :

$$\frac{\partial \tilde{N}_e}{\partial \tilde{t}} + \frac{c}{B_0} \left[(1 - M_1) \tilde{\varphi}, \tilde{N}_e \right] - \frac{n_0}{B_0} [\tilde{A}_{\parallel}, \tilde{U}_e] + n_0 \frac{\partial \tilde{U}_e}{\partial \tilde{z}} = 0, \tag{B7}$$

$$\begin{aligned}
\frac{\partial}{\partial \tilde{t}} \left(m_e \tilde{U}_e - \frac{e}{c} \tilde{A}_{\parallel} \right) + \frac{c}{B_0} \left[(1 - M_1) \tilde{\varphi}, m_e \tilde{U}_e - \frac{e}{c} \tilde{A}_{\parallel} \right] \\
- \frac{1}{B_0} \left[\tilde{A}_{\parallel}, \tilde{T}_{\parallel e} + T_{e0} \frac{\tilde{N}_e}{n_0} \right] - \frac{m_e c}{n_0 T_{0e} B_0} [M_1 \tilde{\varphi}, \tilde{Q}_{\perp e}]
\end{aligned}$$

$$+ \frac{\partial}{\partial \tilde{z}} \left(\tilde{T}_{\parallel e} + T_{0e} \frac{\tilde{N}_e}{n_0} - e(1 - M_1) \tilde{\varphi} \right) = 0, \quad (\text{B8})$$

where we also made use of the relation $\tilde{T}_{\perp e} = -(T_{0e}/B_0)\tilde{B}_z$. We consider then the system resulting from Eqs. (B7)-(B8) upon neglecting the perpendicular heat flux, i.e. setting $\tilde{Q}_{\perp e} = 0$. Introducing the field $\tilde{\phi} = (1 - M_1)\tilde{\varphi} = -(1 - M_1)M_2^{-1}(T_{0e}/e)(\tilde{N}_e/n_0)$, the resulting system can be written as

$$\begin{aligned} & \frac{\partial g_0}{\partial \tilde{t}} + \frac{c}{B_0} [\tilde{\phi}, g_0] - \frac{v_{the}}{B_0 \sqrt{2}} [\tilde{A}_{\parallel}, g_1] \\ & + \frac{v_{the}}{\sqrt{2}} \frac{\partial}{\partial \tilde{z}} \left(g_1 + \frac{v_{the}}{\sqrt{2}} \frac{e \tilde{A}_{\parallel}}{T_{0e} c} \right) = 0, \quad (\text{B9}) \\ & \frac{\partial g_1}{\partial \tilde{t}} + \frac{c}{B_0} [\tilde{\phi}, g_1] - \frac{v_{the}}{B_0} [\tilde{A}_{\parallel}, g_2] \\ & - \frac{v_{the}}{\sqrt{2} B_0} [\tilde{A}_{\parallel}, g_0] + \frac{v_{the}}{\sqrt{2}} \frac{\partial}{\partial \tilde{z}} \left(\sqrt{2} g_2 + g_0 - \frac{e \tilde{\phi}}{T_{0e}} \right) = 0, \quad (\text{B10}) \end{aligned}$$

where

$$\begin{aligned} g_0 &= \frac{\tilde{N}_e}{n_0}, & g_1 &= \sqrt{2} \frac{\tilde{U}_e}{v_{the}} - \sqrt{2} \frac{e}{m_e v_{the} c} \tilde{A}_{\parallel}, \\ g_2 &= \frac{\tilde{T}_{\parallel e}}{\sqrt{2} T_{0e}} \end{aligned} \quad (\text{B11})$$

are the first three moments of the generalized perturbed distribution function \tilde{g}_e with respect to the Hermite polynomials in the variable $\sqrt{2}\tilde{v}/v_{the}$.

Because the field $\tilde{\phi} = -(1 - M_1)M_2^{-1}(T_{0e}/e)(\tilde{N}_e/n_0)$ depends on $\tilde{N}_e/n_0 = g_0$ by means of an operator which is linear, symmetric and independent on the v coordinate, Eqs. (B9) and (B10) fall in the framework of the theory on Hamiltonian closures described in Ref. [27] (compare Eqs. (B9)-(B10) with Eqs. (27) and (28) of Ref. [27] keeping in mind that, in Ref. [27], the constant v_{the} is defined as $v_{the} = \sqrt{T_{0e}/m_e}$ and consequently differs by a factor $\sqrt{2}$ with respect to the constant v_{the} used in the present paper).

According to the results of Ref. [27], the system (B9)-(B10), complemented by the relations (B4), is Hamiltonian if it is closed by imposing a relation $g_2 = \alpha g_1$, with constant α . In particular, if we impose $g_2 = 0$ (which corresponds to the isothermal closure for the parallel temperature), the system is Hamiltonian and, when written in terms of dimensionless variables according to Eqs. (A1), it corresponds namely to the two-field gyrofluid model (30)-(31), complemented by the relations (32) and (33).

This Hamiltonian derivation automatically takes into account the additional subdominant term $[B_z, (2\delta^2/\beta_e)\Delta_{\perp} A_{\parallel}]$, which had to be added a posteriori in the derivation presented in Sec. II B.

According to the prescription of Ref. [27], the Hamiltonian functional of the two-field model is obtained by replacing, in the Hamiltonian (B5) of the parent drift-kinetic model, the following truncated expansion for \tilde{g}_e :

$$\tilde{g}_e = \tilde{F}_{eqe} \left(\frac{\tilde{N}_e}{n_0} + \sqrt{2} \frac{\tilde{v}}{v_{the}} \left(\sqrt{2} \frac{\tilde{U}_e}{v_{the}} - \sqrt{2} \frac{e}{m_e v_{the} c} \tilde{A}_{\parallel} \right) \right). \quad (\text{B12})$$

In terms of the appropriate dimensionless variables, this yields the Hamiltonian (44). Concerning the Poisson bracket, we remark first that the system (B9)-(B10), closed by the relation $g_2 = 0$, can be written as

$$\begin{aligned} & \frac{\partial g_m}{\partial \tilde{t}} + \frac{c}{B_0} [\tilde{\phi}, g_m] - \frac{v_{the}}{\sqrt{2} B_0} [\tilde{A}_{\parallel}, W_{mn} g_n] + \frac{v_{the}}{\sqrt{2}} \frac{\partial}{\partial \tilde{z}} W_{mn} g_n \\ & - \delta_{m1} \frac{v_{the}}{\sqrt{2}} \frac{\partial}{\partial \tilde{z}} \frac{e \tilde{\phi}}{T_{0e}} + \delta_{m0} \frac{v_{the}^2}{2} \frac{\partial}{\partial \tilde{z}} \frac{e \tilde{A}_{\parallel}}{c T_{0e}}, \quad m = 0, 1, \end{aligned} \quad (\text{B13})$$

where sum over repeated indices is understood and where the matrix W , with elements W_{mn} , is given by

$$W = \begin{pmatrix} 0 & 1 \\ 1 & 0 \end{pmatrix}. \quad (\text{B14})$$

Following Ref. [27], it is then convenient to introduce the variables $\mathcal{G}_i = \sum_{j=0}^1 U_{ij}^T g_j$, for $i = 0, 1$, where U^T is the transpose of the orthogonal matrix U that diagonalizes the matrix W . In the case of the present model we obtain

$$\mathcal{G}_0 = \frac{g_0}{\sqrt{2}} + \frac{g_1}{\sqrt{2}}, \quad (\text{B15})$$

$$\mathcal{G}_1 = \frac{g_0}{\sqrt{2}} - \frac{g_1}{\sqrt{2}}. \quad (\text{B16})$$

Note that $\mathcal{G}_0 = -G_-/(\sqrt{2}\delta)$ and $\mathcal{G}_1 = G_+/(\sqrt{2}\delta)$, where G_{\pm} are the normal fields introduced in Sec. II E.

In terms of the variables $\mathcal{G}_{0,1}$, the Poisson bracket is given, according to Ref. [27], by

$$\begin{aligned} \{F, G\} &= \sum_{i=0}^1 \left(\frac{\sqrt{2}c}{e B_0 n_0} \int d^3 \tilde{x} \mathcal{G}_i [F_{\mathcal{G}_i}, G_{\mathcal{G}_i}] \right. \\ & \left. - \frac{v_{the}}{\sqrt{2} T_{0e} n_0} \lambda_i \int d^3 \tilde{x} F_{\mathcal{G}_i} \frac{\partial}{\partial \tilde{z}} G_{\mathcal{G}_i} \right), \end{aligned} \quad (\text{B17})$$

where $\lambda_0 = 1$ and $\lambda_1 = -1$ are the eigenvalues of the matrix W .

By mapping the Poisson bracket (B17) to the variables N_e and A_e , with the appropriate normalization, one can retrieve the Poisson bracket (45).

-
- [1] F. C. M. Faganello and F. Pegoraro, *Phys. Rev. Lett.* **101**, 175003 (2008).
- [2] F. Sahraoui, M. L. Goldstein, P. Robert, and Y. U. Khotyaintsev, *Phys. Rev. Lett.* **102**, 231102 (2009).
- [3] C. H. K. Chen, T. S. Horbury, A. A. Schekochihin, R. T. Wicks, O. Alexandrova, and J. Mitchell, *Phys. Rev. Lett.* **104**, 255002 (2010).
- [4] O. Alexandrova, C. Lacombe, A. Mangeney, R. Grappin, and M. Maksimovic, *Astrophys. J.* **760**, 121 (2012).
- [5] C. H. K. Chen, S. Boldyrev, Q. Xia, and J. C. Perez, *Phys. Rev. Lett.* **110**, 225002 (2013).
- [6] F. Sahraoui, S. Y. Huang, G. Belmont, M. L. Goldstein, A. Réтино, P. Robert, and J. De Patoul, *Astrophys. J.* **777**, 15 (2013).
- [7] S. S. Cerri, F. Califano, F. Jenko, D. Told, and F. Rincon, *Astrophys. J. Lett.* **822**, L12 (2016).
- [8] L. Z. Hadid, F. Sahraoui, and S. Galtier, *Astrophys. J.* **838**, 9 (2017).
- [9] C. H. K. Chen, L. Leung, S. Boldyrev, B. A. Maruca, and S. D. Bale, *Geophys. Res. Lett.* **41**, 8081 (2014).
- [10] A. A. Schekochihin, S. C. Cowley, W. Dorland, G. W. Hammett, G. G. Howes, E. Quataert, and T. Tatsuno, *Astrophys. J. Suppl.* **182**, 310 (2009).
- [11] S. Boldyrev and J. C. Perez, *Astrophys. J. Lett.* **758**, L44 (2012).
- [12] R. Fitzpatrick and F. Porcelli, *Phys. Plasmas* **11**, 4713 (2004).
- [13] R. Fitzpatrick and F. Porcelli, *Phys. Plasmas* **14**, 049902 (2007).
- [14] E. Tassi, P. J. Morrison, D. Grasso, and F. Pegoraro, *Nucl. Fusion* **50**, 034007 (2010).
- [15] C. T. Hsu, R. D. Hazeltine, and P. J. Morrison, *Phys. Fluids* **29**, 1480 (1986).
- [16] T. Passot, P. L. Sulem, and E. Tassi, *J. Plasma Phys.* **83**, 715830402 (2017).
- [17] C. H. K. Chen and S. Boldyrev, *Astrophys. J.* **842**, 122 (2017), arXiv:1705.08558v1 [physics-space-ph].
- [18] N. H. Bian and E. P. Kontar, *Phys. Plasmas* **17**, 062308 (2010).
- [19] T. J. Schep, F. Pegoraro, and B. N. Kuvshinov, *Phys. Plasmas*, 2843 (1994).
- [20] A. Brizard, *Phys. Fluids B* **4**, 1213 (1992).
- [21] S. S. Cerri and F. Califano, *New J. Phys.* **19**, 025007 (2017).
- [22] L. Franci, S. Landi, L. Matteini, A. Verdini, and P. Hellinger, *Astrophys. J.* **833**, 91 (2016), arXiv:1610.05158 [physics.space-ph].
- [23] B. Scott, *Phys. Plasmas* **17**, 102306 (2010).
- [24] P. B. Snyder and G. W. Hammett, *Phys. Plasmas* **8**, 3199 (2001).
- [25] E. Tassi, P. L. Sulem, and T. Passot, *J. Plasma Phys.* **82**, 705820601 (2016).
- [26] P. L. Sulem, T. Passot, D. Laveder, and D. Borgogno, *Astrophys. J.* **818**, 66 (2016).
- [27] E. Tassi, *Annals of Physics* **362**, 239 (2015).
- [28] T. Passot and P. L. Sulem, *Phys. Plasmas* **14**, 082502 (2007).
- [29] D. Borgogno, D. Grasso, F. Porcelli, F. Califano, and D. Pegoraro, F. Farina, *Phys. Plasmas* **12**, 032309 (2005).
- [30] D. Biskamp, E. Schwarz, and J. F. Drake, *Phys. Plasmas* **4**, 1002 (1997).
- [31] E. Tassi, *Eur. Phys. J. D* **71**, 269 (2017).
- [32] P. J. Morrison, *Rev. Mod. Phys.* **70**, 467 (1998).
- [33] F. L. Waelbroeck, R. D. Hazeltine, and P. J. Morrison, *Phys. Plasmas* **16**, 032109 (2009).
- [34] E. Cafaro, D. Grasso, F. Pegoraro, F. Porcelli, and A. Saluzzi, *Phys. Rev. Lett.* **80**, 4430 (1998).
- [35] U. Frisch, A. Pouquet, J. Léorat, and A. Mazure, *J. Fluid Mech.* **68**, 769 (1975).
- [36] G. Miloshevich, M. Lingam, and P. J. Morrison, *New J. Phys.* **19**, 015007 (2017).
- [37] A. Pouquet, U. Frisch, and J. Léorat, *J. Fluid Mech.* **77**, 321 (1976).
- [38] H. M. Abdelhamid, M. Lingam, and S. M. Mahajan, *Astrophys. J.* **829**, 87 (2016).
- [39] T. Passot and P. L. Sulem, *Astrophys. J. Lett.* **812**, L37 (2015).
- [40] J. Cho, *J. Phys. Conf. Ser.* **719**, 012001 (2016).
- [41] H. Kim and J. Cho, *Astrophys. J.* **801**, 75 (2015).
- [42] S. Galtier and R. Meyrand, *J. Plasma Phys.* **81**, 325810106 (2015).
- [43] L. Franci, S. S. Cerri, F. Califano, S. Landi, E. Papini, A. Verdini, L. Matteini, F. Jenko, and P. Hellinger, *Astrophys. J. Lett.* **850**, L16 (2017), arXiv:1707.06548 [physics.space-ph].
- [44] A. Zocco and A. Schekochihin, *Phys. Plasmas* **18**, 102309 (2011).
- [45] S. Y. Huang, F. Sahraoui, X. H. Deng, J. S. He, Z. G. Yuan, M. Zhou, Y. Pang, and H. S. Fu, *Astrophys. J. Lett.* **789**, L28 (2014).